

## CODING OF IMAGE CONTRAST IN CENTRAL VISUAL PATHWAYS OF THE MACAQUE MONKEY

GARY SCLAR,<sup>1</sup> JOHN H. R. MAUNSELL<sup>2</sup> and PETER LENNIE<sup>3\*</sup>

<sup>1</sup>Center for Visual Science and Departments of <sup>2</sup>Physiology and <sup>3</sup>Psychology,  
University of Rochester, Rochester, NY 14627, U.S.A.

(Received 27 December 1988; in revised form 7 June 1989)

**Abstract**—Measurements of contrast sensitivity were obtained from isolated neurons in the lateral geniculate nucleus, striate cortex, and middle temporal visual area of macaque monkeys. Between the lateral geniculate nucleus and the middle temporal area contrast sensitivity functions become progressively steeper. Furthermore, many neurons in the middle temporal area are more sensitive than any cell encountered in early stages. Measurements made with stimuli of different sizes show that this high sensitivity depends on areal summation across the receptive field.

Contrast      Single-unit      Macaque      Lateral geniculate nucleus      Striate cortex      Middle  
temporal visual area

### INTRODUCTION

Neurons in the visual pathway give graded responses to different levels of stimulus contrast. For retinal ganglion cells and neurons in the dorsal lateral geniculate nucleus (LGN) these responses provide a relatively faithful representation of image contrast, but it is not clear that the graded responses of cells at higher levels contain much information about contrast. Many neurophysiological and behavioral experiments suggest that the responses of neurons in higher cortical visual areas encode increasingly complex features of stimuli (see Maunsell & Newsome, 1987). Presumably this more complex information is represented at the expense of information about stimulus contrast. Barlow (1972), for example, has suggested that the amplitude of response might represent the probability that a particular "trigger feature" is present.

We have examined how neurons at different stages in the visual pathway of macaque monkey respond to variations in the contrast of stimuli. We have characterized the contrast-response relationships of neurons in the LGN, striate cortex (V1) and the middle temporal visual area (MT), and have analyzed the differences between them. We chose these sites because they represent distinctly different levels within a hierarchy of visual processing.

We distinguish cells in the two major parallel subdivisions of the thalamo-cortical pathway: the parvocellular (*P*) and magnocellular (*M*) streams. *P*-cells in the LGN project principally to layer 4C $\beta$  of V1 and to a lesser extent to layer 4A (Hubel & Wiesel, 1972). Within V1 the *P* stream leads mainly to layers 2 and 3 (Lund & Boothe, 1975), but subsequent stages of analysis are less clearly identified. *M*-cells in the LGN project to layer 4C $\alpha$  of V1. Outputs from this layer lead mainly to layer 4B (Fitzpatrick, Lund & Blasdel, 1985), and from there to MT (Lund, Lund, Hendrickson, Bunt & Fuchs, 1976), although layer 4C $\alpha$  also sends axons to superficial layers in V1. Thus for both pathways, but the *M* pathway in particular, we can examine how contrast is encoded at different levels.

### METHODS

These experiments were undertaken on 30 *Macaca fascicularis* weighing between 2.5 and 6.0 kg. In all but four of the animals the measurements used in the present work were collected during the course of experiments reported by Derrington and Lennie (1984); DePriest, Sclar and Lennie (1988); Lennie, Krauskopf and Sclar (1989) and Sclar, Lennie and DePriest (1989).

#### *Preparation for recording*

Anesthesia was induced with ketamine hydrochloride (10 mg kg<sup>-1</sup> i.m.), or occasionally suf-

\*To whom correspondence should be addressed.

entanil citrate (Sufenta, Janssen, 8–10  $\mu\text{g kg}^{-1}$  i.m.). Supplementary doses of anesthetic were provided as necessary during surgery. Cannulae were placed in the saphenous veins of both legs and in the trachea. The head was mounted in a stereotaxic holder and a small craniotomy was made either above the LGN, over the foveal representation of V1, or over the superior temporal sulcus. Stainless steel screws were implanted along the sagittal suture for recording the EEG, and the ECG was monitored through electrodes in the forelimbs. Body temperature was measured with a subscapular thermistor, and held close to 37 deg with a thermostatically-controlled heating pad. After an electrode carrier had been placed in the recording position the craniotomy was covered with warm agar and sealed with wax.

In early experiments on LGN, anesthesia was maintained during recordings with small injections of Nembutal; in later experiments an infusion of sufentanil (initially 2  $\mu\text{g kg}^{-1} \text{hr}^{-1}$ ) in lactated Ringer's solution was used. In both cases a muscle relaxant was infused to immobilize the eyes (vecuronium bromide, 100  $\mu\text{g kg}^{-1} \text{hr}^{-1}$  or pancuronium bromide, 60  $\mu\text{g kg}^{-1} \text{hr}^{-1}$ ). The monkey was ventilated at 30 strokes  $\text{min}^{-1}$  at a tidal volume adjusted to keep the end-tidal  $\text{CO}_2$  close to 33 mm Hg. Mydriasis and cycloplegia were obtained with atropine sulfate drops (1%) and the corneas were protected with contact lenses that contained artificial pupils 2.5 mm in diameter. Supplementary lenses were used when necessary to refract the animal for the 2.7 or 5.4 m viewing distances used. Lenses were chosen initially through ophthalmoscopic examination, and the refraction was checked using a neuron with a small receptive field by finding what power of lens permitted resolution of the highest spatial frequencies.

#### *Recording and visual stimulation*

Action potentials of isolated units were recorded with glass-insulated tungsten electrodes, amplified and converted to standard pulses that were counted by computer. The receptive field (of the dominant eye in the case of cortical units) was projected on the face of a television display (160 frames  $\text{sec}^{-1}$ , 200  $\text{cd m}^{-2}$  for the early experiments on the LGN; 120 frames  $\text{sec}^{-1}$  interlaced, 120  $\text{cd m}^{-2}$  for all the others). The luminance of the display used in the early experiments varied linearly with applied voltage; the frame-buffer controller used in the later experiments compensated for a non-

linearity in the display. Contrast could be controlled to better than 1 part in 512. All cells were driven by achromatic sinusoidal gratings moving steadily across the receptive field. For work on LGN these were horizontal; for work on cortex they were set to the preferred orientation and direction of movement of the cell being studied. The preferred direction and rate of movement were determined by listening to the output of an audio monitor; the preferred spatial frequency was found by measuring responses to at least five presentations of each of a series of gratings of different spatial frequencies. The preferred spatial frequency was then used in determining the relationship between stimulus contrast and amplitude of response. Stimuli of different contrasts were presented in a pseudo-random order.

#### *Data analysis*

Average response histograms were constructed from the accumulated impulse counts, and from these we calculated the amplitudes of the average discharge rate ( $f_0$ ) and the component at the frequency of stimulation ( $f_1$ ). The amplitude of  $f_1$  was used as the measure of response for simple cells in V1 and for neurons in LGN; the amplitude of  $f_0$  was used for complex cells in V1 and for all cells in MT. These measures capture the most substantial components of the responses of the different classes of cells to moving gratings.

To compare the properties of cells at different levels in the visual pathway we need an economical and consistent method to describe their contrast-response relationships. We have found that in all three regions studied these relationships are well-characterized by the expression

$$R = R_{\max} c^n / (c^n + c_{50}^n) + M; \quad (1)$$

where  $R$  is the amplitude of the discharge,  $c$  is contrast and  $R_{\max}$ ,  $c_{50}$  and  $n$  denote respectively the maximum attainable response, the contrast at which the response reaches half its maximum value, and the exponent that determines the steepness of the curve.  $M$  represents the rate of the spontaneous discharge. This function has previously been shown to provide a good fit to contrast response functions from visual cortex in the cat and monkey (Albrecht & Hamilton, 1982). In psychophysical experiments contrast sensitivity is defined as the reciprocal of the lowest detectable contrast. An analogous physiological measure would be the reciprocal of the contrast required for a criterion response;

while recognizing that this would be jointly determined by  $R_{\max}$ ,  $c_{50}$  and  $n$ , we have simply used  $c_{50}$  as an index of it.

### Reconstruction of electrode tracks

Small lesions were made at specified positions in each penetration by passing current through the tip of the electrode. At the end of the experiment the animal was given an overdose of Nembutal and was perfused with 0.9% saline in neutral phosphate buffer, followed either by a solution of 1.25% paraformaldehyde and 2.5% glutaraldehyde or 10% formalin. Brains were blocked and sectioned, and alternate sections were usually stained for thionin and cytochrome oxidase. The positions of recording sites were deduced from the reconstructed electrode tracks. When recordings were made in MT a series of sections was also stained for myelin (Gallyas, 1979), and the borders of MT were established from its characteristic myelination (Van Essen, Maunsell & Bixby, 1981).

## RESULTS

### General features of the contrast-response relationships

Figures 1A and B show contrast-response relationships for two parvocellular neurons (*P*-cells) in the LGN. Figures 1C and D show the corresponding relationships for two magnocellular neurons (*M*-cells). Figures 1A and C describe the behavior of relatively insensitive cells, as defined by values of  $c_{50}$  (see Methods); Figs 1B and D represent more sensitive ones. *M*- and *P*-cells are clearly distinguished by their responses to low-contrast stimuli, but the shapes of the curves are similar—indeed they can be described satisfactorily by the same function (see below).

Contrast-response relationships obtained from cells in V1 resemble those obtained from neurons in LGN. Figures 2A and B show curves for simple cells, and Figs 2C and D curves for complex cells. For the simple cells the amplitude of the  $f_1$  is the measure of response; for the complex cells the value of  $f_0$  is the measure (see Methods). As in Fig. 1, the left-hand graphs (Figs 2A and C) characterize relatively insensitive cells and the right-hand graphs sensitive ones. The relatively sensitive cells (Figs 2B and D) showed more profound saturation and gave graded responses to a smaller range of contrasts (had smaller dynamic range) than did neurons in LGN.

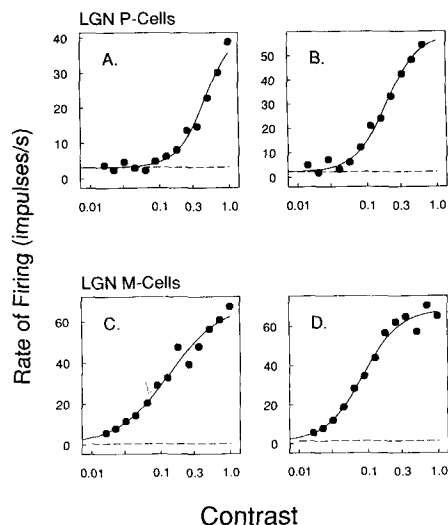


Fig. 1. Contrast-response functions obtained from neurons in the parvocellular layers (A, B) and magnocellular layers (C, D) of the LGN. All panels show the amplitude of the  $f_1$  component of response evoked by moving gratings of optimal spatial frequency. A and C are examples from the least sensitive thirds of their respective populations; B and D are examples from the most sensitive thirds. The smooth curves drawn through the points are the best-fitting solutions to equation (1). The dashed lines represent average spontaneous activity for each neuron. Each point in Figs 1-3 represents the average of responses from 20 stimulus presentations.

The contrast-response relationships for neurons in MT (Fig. 3) share the general characteristics of those in V1 and the LGN, but MT neurons typically responded to lower contrasts than did most neurons in V1 and had even narrower dynamic ranges, so that for many cells the responses saturated at low contrast (cf. Figs 3B and D). The contrast-response relationship shown in Fig. 3A was obtained from an unusually insensitive cell.

The smooth curves drawn through the points in Figs 1-3 are the best-fitting solutions to equation (1) found using the routine STEPIT to obtain the least-squares error, with the parameters  $R_{\max}$ ,  $c_{50}$ ,  $n$  and  $M$  allowed to vary freely. Equation (1) describes most of the contrast-response relationships well: median r.m.s. errors of the fitted curves were 14% for *P*-cells, 6% for *M*-cells, 6% for neurons in V1 and 9% for neurons in MT. Table 1 shows the median values of  $R_{\max}$ ,  $c_{50}$  and  $n$  for neurons in each of the structures examined, and Figs 4-6 show the corresponding distributions. The distributions of  $R_{\max}$  (Fig. 4) do not distinguish *M*- and *P*-cells, neither do they distinguish neurons in V1 and MT, but they do distinguish neurons in

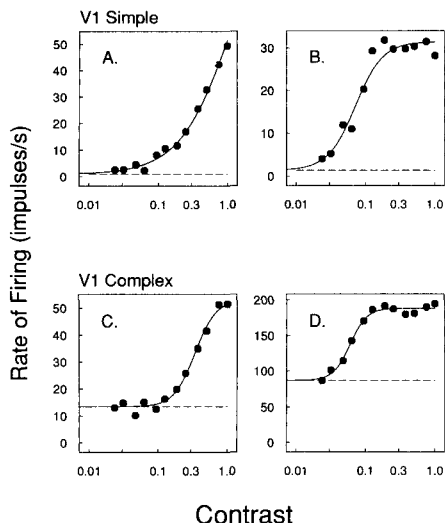


Fig. 2. Contrast-response functions obtained from two simple cells (A, B) and two complex cells (C, D) in V1. For simple cells the graphs show the amplitude of the  $f_1$  component of response evoked by moving gratings of the optimal spatial frequency and orientation; for complex cells the graphs show the amplitude of  $f_0$ . A and C are examples from the least sensitive thirds of their respective populations; B and D are from the most sensitive thirds.

cortex from those in the LGN: the median value of  $R_{\max}$  in both cortical areas is less than three-quarters that in the LGN.

The distributions of  $c_{50}$  for  $P$ - and  $M$ -cells

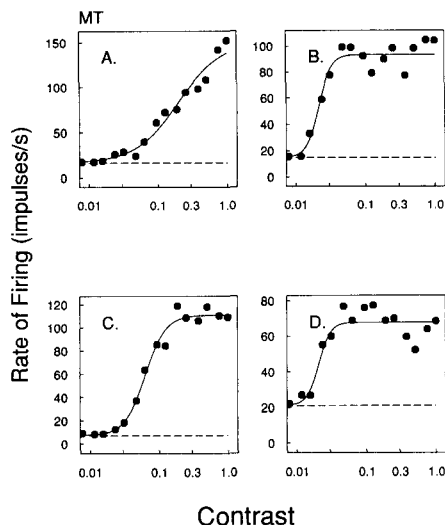


Fig. 3. Contrast-response functions obtained from four neurons in MT. All panels show the amplitude of the  $f_0$  component of response evoked by a moving grating of optimal spatial frequency and orientation. The measurements shown in A were obtained from one of the least sensitive neurons encountered in MT. The average of the preferred temporal frequencies for MT units, which were judged by listening to responses, was 5.4 c/sec. The average of preferred spatial frequencies, which were measured, was 0.7 c/deg.

Table 1. Median values for the parameters of equation (1) calculated for each of the structures studied

Visual structure	(units)	$R_{\max}$	$c_{50}$	$n$
Parvocellular LGN	(102)	48.7	0.50	1.6
Magnocellular LGN	(26)	52.7	0.11	1.2
V1	(86)	27.4	0.33	2.4
MT	(63)	36.0	0.07	3.0

(Fig. 5) reflect the well-established difference between the contrast sensitivities of the two classes of cells. Median values differ by a factor of almost 5. Although the distribution for V1 resembles the envelope of the combined distributions for  $P$ - and  $M$ -cells, it would be unwarranted to conclude that the more sensitive cells in V1 receive input from  $M$ -cells and the less-sensitive from  $P$ -cells. Since neurons in LGN have no true threshold and give graded responses to even the lowest contrasts (Derrington & Lennie, 1984), V1 neurons driven solely by  $P$ -cells could achieve low values of  $c_{50}$  through summation of signals from multiple inputs. This point is illustrated more clearly by a comparison of the distribution of  $c_{50}$  for cells in MT with those for the LGN and V1: 29% (18/63) of the MT cells examined had values of  $c_{50}$  lower than any seen in V1 or LGN.

Because the samples from the LGN, V1 and MT were not perfectly matched for eccentricity, we must consider whether differences in eccentricity (and corresponding differences in recep-

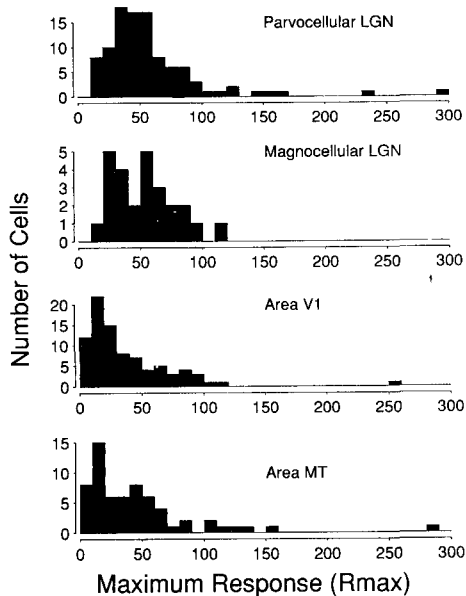


Fig. 4. Distributions of the saturating response ( $R_{\max}$ ) for neurons in parvocellular LGN, magnocellular LGN, V1 and MT.

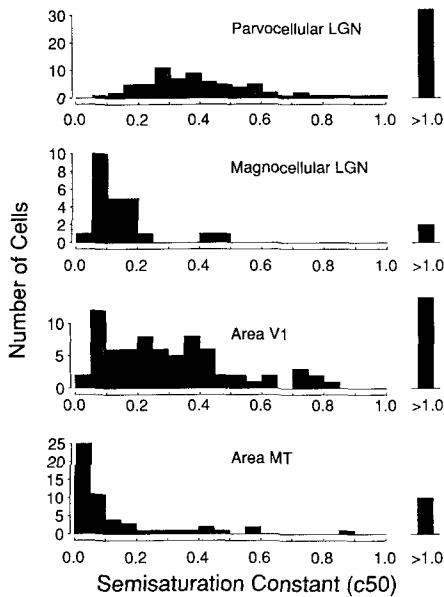


Fig. 5. Distributions of the semisaturation constant ( $c_{50}$ ) for neurons in parvocellular LGN, magnocellular LGN, V1 and MT.

tive field size) could account for the different distributions of  $c_{50}$ . LGN receptive fields were sampled from 0 to 40 deg eccentricity, with most from the central 10 deg. V1 receptive fields lay within 3 deg of the center of the fovea, and receptive field centers in MT were distributed around 10 deg eccentricity (3 deg SD). Two lines of evidence argue against eccentricity being a major factor. First, the populations of cells in LGN and MT were drawn mostly from the same range of eccentricities, although their distributions of  $c_{50}$  differed most. Second, there is clear evidence from work on cat, where the relationship between contrast sensitivity and eccentricity has been studied systematically, that eccentricity *per se* has no effect on peak contrast sensitivity (Linsenmeier, Frishman, Jakiela & Enroth-Cugell, 1982). Later we examine how differences in receptive field area contribute to differences in contrast–response functions.

The exponent  $n$  determines the steepness of the contrast–response relationship, larger values being associated with steeper slopes. Figure 6 shows that the exponents for *M*-cells and *P*-cells lie between 1 and 2 (denoting a relationship in which response varies nearly linearly with contrast until contrast approaches  $c_{50}$ ), but that substantial numbers of neurons in both V1 and MT have larger exponents, and therefore steeper contrast–response relationships. Albrecht and Hamilton (1982) reported similar values for contrast sensitivity in V1, but their

median values were slightly higher for  $c_{50}$  and lower for exponents. This disagreement may reflect differences in the proportions of the neurons sampled in each cortical layer.

### Summation of signals in MT

At corresponding eccentricities, receptive fields of neurons in MT, as defined by the “minimum response field” (Pettigrew, Nikara & Bishop, 1968), have about 100 times greater area than receptive fields in V1 and LGN (Dow, Snyder, Vautin & Bauer, 1981; Gattass & Gross, 1981; Hubel & Wiesel, 1974; Van Essen et al., 1981; Van Essen, Newsome & Maunsell, 1984). Neurons in MT therefore presumably accumulate signals from many V1 cells that sample the region covered by the receptive field. We can obtain some idea of how these signals are combined by examining contrast–response relationships for stimuli of different sizes falling within the receptive fields of neurons in MT.

We measured contrast–response relationships in 21 neurons in MT with gratings at a range of sizes from the dimensions of a receptive field in the LGN to larger than the receptive field of the MT neuron. In each case the spatial and temporal frequencies of the grating were fixed at the optimal values, and the grating remained centered over the middle of the receptive field as size was varied. Where a grating was smaller than the receptive field the surrounding area

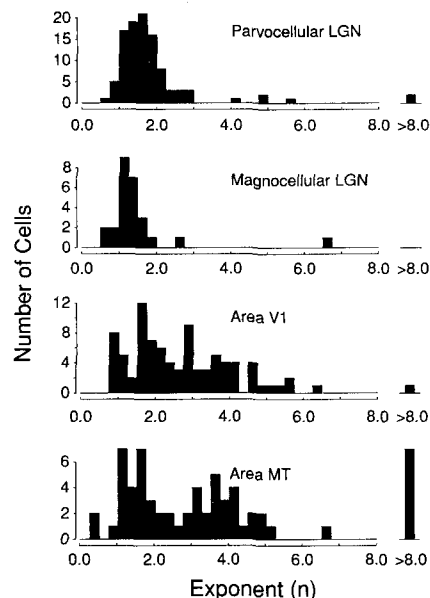


Fig. 6. Distributions of the exponent ( $n$ ), which controls the steepness of the contrast response function at intermediate contrasts, for neurons in parvocellular LGN, magnocellular LGN, V1 and MT.

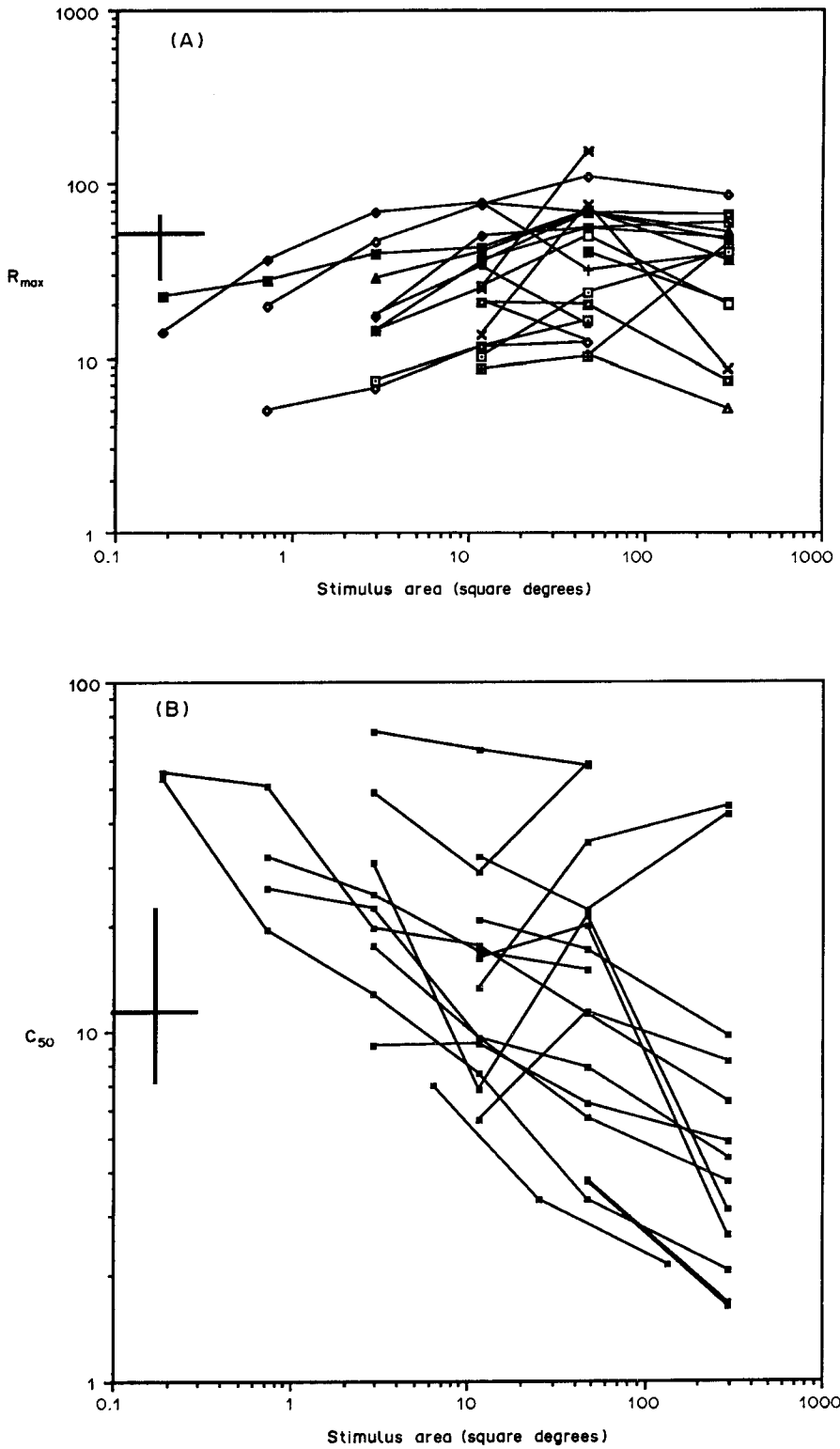


Fig. 7. Spatial summation within the receptive fields of neurons in MT. (A) Change of  $R_{max}$  with stimulus size. (B) Change of  $c_{50}$  with stimulus size. In each part of the figure the crossed lines indicate the ranges within which would fall points for  $M$ -cells in the LGN: the horizontal bar shows the mean receptive field diameter  $\pm 1$  SD; the vertical bar shows the median  $R_{max}$  (A) or  $c_{50}$  (B)  $\pm$  a corresponding proportion of that distribution.

was left uniformly illuminated at the average luminance of the grating.

Reductions in stimulus size from its optimum had for most cells a negligible effect on the maintained discharge and the exponent  $n$ , but brought about a modest reduction in  $R_{\max}$  and a marked increase in  $c_{50}$ . Figure 7A shows, for the group of neurons in MT, how  $R_{\max}$  varied with the areas covered by the gratings; Fig. 7B shows the corresponding variation in  $c_{50}$ . Up to six different sizes of grating were used on each neuron. The crossed bars in Fig. 7A and B indicate the region within which would fall most  $M$ -cells in the LGN (see caption for details). For most cells,  $R_{\max}$  grew gradually with stimulus size up to the size of the minimum response field and declined slightly thereafter. For all but a few cells  $c_{50}$  varied almost inversely with the square-root of stimulus size over the range studied. Some form of spatial summation evidently extended beyond the minimum response field (range 11–87 deg<sup>2</sup>), for  $c_{50}$  usually continued to decline as the stimulus became larger than this region.

## DISCUSSION

### *M and P pathways*

Our analysis has characterized more precisely than earlier work the striking difference between the contrast responses of  $M$ - and  $P$ -cells, and has provided a similarly detailed account of the contrast responses of cortical neurons. The high contrast sensitivities of individual neurons in MT confirm expectations based on earlier observations. Because the major projection from V1 to MT arises from layer 4b (Lund et al., 1976; Maunsell & Van Essen, 1983c), which itself receives input from layer 4C $\alpha$  (Lund, 1987; Lund et al., 1976), several reports have suggested that MT is driven primarily via the  $M$ -cells in the LGN (DeYoe & Van Essen, 1988; Hubel & Livingstone, 1987; Maunsell, 1987; Maunsell & Van Essen, 1983a). Blasdel and Fitzpatrick (1984) found that layer 4B neurons have contrast threshold comparable to those found in layer 4C $\alpha$ . Hawken and Parker (1984) reported a wide range of contrast sensitivities in layer 4B, but a more recent study (Hawken, Parker & Lund, 1988) found that the direction selective neurons, which are the ones that project to MT (Movshon & Newsome, 1984), have distinctly higher contrast sensitivity than other neurons. The high contrast sensitivities of neurons in MT are also consistent with the obser-

vation of Tootell, Hamilton and Switkes (1988) that visual stimulation with gratings of low contrast (8%) leads to a preferential uptake of 2-deoxyglucose in layers 4C $\alpha$ , 4B and 6.

While close correspondences between contrast sensitivities of cortical neurons and those of  $P$ -cells and  $M$ -cells provide useful clues about the flow of information in the geniculocortical pathway, they do not warrant the inference that sensitive neurons are driven by  $M$ -cells and less sensitive ones by  $P$ -cells. Summation of signals from several  $P$ -cells could provide a cortical neuron with substantially higher sensitivity than that possessed by any of its inputs. Conversely, an insensitive cortical neuron might receive attenuated signals from  $M$ -cells. Similar problems exist for any attempt to infer the relative effectiveness of inputs from  $P$ - and  $M$ -cells from the distribution of visual sensitivity along other stimulus dimensions.

### *Spatial summation*

Our observations on neurons in MT provide direct evidence for summation of inputs. When stimuli filled their excitatory receptive fields, many MT neurons had values of  $c_{50}$  smaller than those of any neuron studied in the LGN or V1. Sensitivity declined rapidly as stimulus size was reduced, and gratings confined to regions comparable in size to the center of  $M$ -cell receptive fields yielded values of  $c_{50}$  close to those found for  $M$ -cells in the LGN. The high contrast sensitivity seen in MT could easily be generated by summing inputs from many  $P$ -cells, but the anatomical evidence discussed above makes it more likely to depend on summation from  $M$ -cells. Because an individual receptive field in MT can span an area that includes as many as 10,000  $M$ -cells, there is great potential for summation of inputs.

The simplest mechanism for spatial summation would add inputs linearly. With a mechanism of this sort the sensitivity of MT neurons would be expected to be proportional to the area of the stimulus. However, our results show that sensitivity increases in proportion to the square root of stimulus area (Fig. 7). Although the distribution of contrast sensitivity within receptive fields in MT has not been explored quantitatively, a markedly inhomogeneous distribution seems unlikely because sensitivities to properties like direction of motion or binocularly disparity are uniform across the minimum response field (Maunsell & Van Essen, 1983b; Zeki, 1974). We therefore need to consider why

the recruitment of regions of apparently uniform sensitivity does not result in sensitivity being proportional to stimulus area.

Spatial summation within a receptive field is valuable because it improves the detectability of stimuli that fill the summation area. Signals that arise from these stimuli are usually detected in the presence of some background activity (noise), which grows with stimulus area more slowly than do the signals. Noise in the early stages of the visual pathway is well represented by a Poisson process (Barlow and Levick, 1969), so its amplitude grows as the square-root of the number of active inputs. The signal grows in proportion to the number of active inputs, so the signal-to-noise ratio grows in proportion to the square root of stimulus area. However, spatial summation over a large region also introduces potential problems. First, the cell is an inefficient detector of stimuli smaller than the summation area because in this situation all inputs contribute noise while few contribute signal. Second, if all inputs to the neuron are driven by noise, the cell is liable to have a high rate of spontaneous firing that reduces the working range available for responses. The form of spatial summation found in neurons in MT may reflect the action of mechanisms that are designed to cope with these problems.

The first problem can be dealt with by imposing a threshold that must be exceeded before any input can drive the MT cell. This threshold would be set above the level of the spontaneous activity in the input. The MT neuron would then behave as if it were connected only to the parts of its minimum response field that were activated by contrast stimuli. This would improve the detectability of small stimuli by eliminating noise from regions of the minimum response field that provided no signal. The second problem can be solved by a mechanism that adjusts the gain of the active inputs to maintain responses within the working range of the neuron. Such a mechanism might resemble the automatic gain control seen in the retina, and would regulate the gain of the MT neuron in inverse proportion to the level of activity at its inputs. Thus as more inputs are recruited by enlargement of a stimulus, the gain is reduced. To account for observation that  $c_{50}$  falls as the square-root of stimulus area, the gain would have to decline as the square-root of stimulus area. This might be expected were gain regulated primarily by the (Poisson-distributed) noise in the active inputs. Together the

threshold mechanism and the gain control would provide elegant means to optimize the sensitivity of an MT neuron for the stimuli actually present in the receptive field.

### *Representation of contrast*

The representation of image contrast undergoes a pronounced transformation as it ascends the geniculocortical pathway. Responses of neurons in the LGN vary gradually with contrast and can provide information about contrast over a relatively large range. Contrast-response curves become progressively steeper and more readily saturated as one moves to V1 and then to MT, and this greatly reduces the range over which neurons can signal changes in contrast. Steeper contrast-response functions may help cortical neurons sustain high sensitivity to local changes in contrast, but at the expense of a reduced operating range. In V1, contrast adaptation provides some relief from this limitation by moving the operating range of a neuron towards the ambient level of contrast (Sclar et al., 1989), but such adaptation merely underscores the fact that these neurons seem poorly equipped to signal absolute levels of contrast.

Neurons in MT give smoothly graded responses over an extended range to changes in the direction, speed or binocular disparity of moving stimuli (Albright, 1984; Baker, Petersen, Newsome & Allman, 1981; Dubner & Zeki, 1971; Maunsell & Van Essen, 1983a,b; Rodman & Albright, 1987; Zeki, 1974), yet the steep-sloped and rapidly-saturating contrast-response curves of these neurons leave them ill-equipped to convey information about object contrast: providing contrast exceeds some minimum value, neurons respond strongly to objects of a wide range of contrasts. If contrast is a largely irrelevant stimulus dimension, neurons in MT would benefit little from contrast adaptation. We do not know what effect prolonged exposure to high-contrast patterns has on the contrast sensitivity of neurons in MT, although in a recent study on contrast adaptation in V1 Sclar et al. (1989) found that none of four neurons in layer 4B, a major source of input to MT, was affected by prolonged exposure to adapting patterns of high contrast.

The steepness of the contrast-response functions of neurons in MT leads one to expect high contrast sensitivity in perceptual tasks that depend on MT, with little improvement in performance as contrast is raised above threshold.

Psychophysical results do indeed show that when an observer must discriminate direction of motion (Nakayama & Silverman, 1985) or speed (McKee, Silverman & Nakayama, 1986) performance improves little as contrast is raised above threshold. Similarly, Keck, Palella and Pantle (1986) found that the strength of motion after-effects was independent of adapting contrast, provided contrast was above 0.03. These observations are consistent with what we know about MT, though we cannot yet connect them firmly to the behavior of individual neurons.

*Acknowledgements*—Ruth Anne Eatock, Walter Makous and William Merigan kindly commented on the manuscript, and Derryl DePriest, Tara Nealey and Rosanne Shanker helped greatly during some of the experiments. We thank Peter Vamvakias for histological work. This research was supported by NIH grants EY05911, EY04440 and EY01319, and an Alfred P. Sloan Fellowship to J.M.

## REFERENCES

- Albrecht, D. G. & Hamilton, D. B. (1982). Striate cortex of monkey and cat: Contrast response function. *Journal of Neurophysiology*, *48*, 217–237.
- Albright, T. D. (1984). Direction and orientation selectivity of neurons in visual area MT of the macaque. *Journal of Neurophysiology*, *52*, 1106–1130.
- Baker, J., Petersen, S. E., Newsome, W. T. & Allman, J. M. (1981). Visual response properties of neurons in four extrastriate visual areas of the owl monkey (*Aotus trivirgatus*): A quantitative comparison of medial, dorso-medial, dorsolateral and middle temporal areas. *Journal of Neurophysiology*, *45*, 397–416.
- Barlow, H. (1972). Single units and sensation: A neural doctrine for perceptual psychology? *Perception*, *1*, 371–394.
- Barlow, H. B. & Levick, W. R. (1969). Three factors limiting the reliable detection of light by retinal ganglion cells of the cat. *Journal of Physiology, London*, *200*, 1–24.
- Blasdel, G. G. & Fitzpatrick, D. (1984). Physiological organization of layer 4 in macaque striate cortex. *Journal of Neuroscience*, *4*, 880–895.
- DePriest, D. D., Sclar, G. & Lennie, P. (1988). Central limits to chromatic flicker-sensitivity. *Investigative Ophthalmology and Visual Science*, *29*, 326.
- Derrington, A. M. & Lennie, P. (1984). Spatial and temporal contrast sensitivities of neurones in lateral geniculate nucleus of macaque. *Journal of Physiology*, *357*, 291–240.
- DeYoe, E. A. & Van Essen, D. C. (1988). Concurrent processing streams in monkey visual cortex. *Trends in Neuroscience*, *11*, 219–226.
- Dow, B. M., Snyder, A. Z., Vautin, R. G. & Bauer, R. (1981). Magnification factor and receptive field size in foveal striate cortex of the monkey. *Experimental Brain Research*, *44*, 213–228.
- Dubner, R. & Zeki, S. M. (1971). Response properties and receptive fields of cells in an anatomically defined region of the superior temporal sulcus. *Brain Research*, *35*, 528–532.
- Fitzpatrick, D., Lund, J. S. & Blasdel, G. G. (1985). Intrinsic connections of macaque striate cortex: Afferent and efferent connections of lamina 4C. *Journal of Neuroscience*, *5*, 3329–2249.
- Gallyas, F. (1979). Silver staining of myelin by means of physical development. *Neurological Research*, *1*, 203–209.
- Gattass, R. & Gross, C. G. (1981). Visual topography of striate projection zone (MT) in posterior superior temporal sulcus of the macaque. *Journal of Neurophysiology*, *46*, 621–638.
- Hawken, M. J. & Parker, A. J. (1984). Contrast sensitivity and orientation selectivity in Lamina IV of the striate cortex of Old World monkeys. *Experimental Brain Research*, *54*, 367–372.
- Hawken, M. J., Parker, A. J. & Lund, J. S. (1988). Laminar organization and contrast sensitivity of direction-selective cells in the striate cortex of the old world monkey. *Journal of Neuroscience*, *8*, 3541–3548.
- Hubel, D. H. & Livingstone, M. S. (1987). Segregation of form color, and stereopsis in primate area 18. *Journal of Neuroscience*, *7*, 3378–3415.
- Hubel, D. H. & Wiesel, T. N. (1972). Laminar and columnar distribution of geniculate-cortical fibers in the macaque monkey. *Journal of Comparative Neurology*, *146*, 421–450.
- Hubel, D. H. & Wiesel, T. N. (1974). Uniformity of monkey striate cortex: A parallel relationship between field size, scatter, and magnification factor. *Journal of Comparative Neurology*, *158*, 295–305.
- Keck, M. J., Palella, T. D. & Pantle, A. (1986). Motion aftereffect as a function of the contrast of sinusoidal gratings. *Vision Research*, *16*, 187–191.
- Lennie, P., Krauskopf, J. & Sclar, G. (1989). Chromatic mechanisms in striate cortex of macaque. *Journal of Neuroscience* (in press).
- Linsenmeier, R. A., Frishman, L. J., Jakiela, H. G. & Enroth-Cugell, C. (1982). Receptive field properties of X and Y cells in the cat retina derived from contrast sensitivity measurements. *Vision Research*, *22*, 1173–1183.
- Lund, J. S. (1987). Neurons of laminae 4C and 5A. *Journal of Comparative Neurology*, *257*, 60–92.
- Lund, J. S. & Boothe, R. G. (1975). Interlaminar connections and pyramidal neuron organisation in the visual cortex, area 17, of the macaque monkey. *Journal of Comparative Neurology*, *159*, 305–334.
- Lund, J. S., Lund, R. D., Hendrickson, A. E., Bunt, A. H. & Fuchs, A. F. (1976). The origin of efferent pathways from the primary visual cortex area 17, of the macaque monkey as shown by retrograde transport of horseradish peroxidase. *Journal of Comparative Neurology*, *164*, 287–304.
- Maunsell, J. H. R. (1987). Physiological evidence for two visual subsystems. In Vaina, L. M. (Ed.), *Matters of Intelligence* (pp. 59–87). Dordrecht: Reidel.
- Maunsell, J. H. R. & Newsome, W. T. (1987). Visual processing in monkey extrastriate cortex. *Annual Review of Neuroscience*, *10*, 363–401.
- Maunsell, J. H. R. & Van Essen, D. C. (1983a). Functional properties of neurons in the middle temporal visual area of the macaque: I. Selectivity for stimulus direction, speed, and orientation. *Journal of Neurophysiology*, *49*, 1127–1147.
- Maunsell, J. H. R. & Van Essen, D. C. (1983b). Functional properties of neurons in the middle temporal visual area of the macaque: II. Binocular interactions and sensitivity to binocular disparity. *Journal of Neurophysiology*, *49*, 1148–1167.
- Maunsell, J. H. R. & Van Essen, D. C. (1983c). The

- connections of the middle temporal visual area in the macaque and its relationship to a hierarchy of cortical visual areas. *Journal of Neuroscience*, 3, 2563–2586.
- McKee, S. P., Silverman, G. H. & Nakayama, K. (1986). Precise velocity discrimination despite random variations in temporal frequency and contrast. *Vision Research*, 26, 609–619.
- Movshon, J. A. & Newsome, W. T. (1984). Functional characteristics of striate cortical neurons projecting to MT in the macaque. *Society for Neuroscience Abstracts*, 10, 933.
- Nakayama, K. & Silverman, G. H. (1985). Detection and discrimination of sinusoidal grating displacements. *Journal of the Optical Society of America*, A2, 267–274.
- Pettigrew, J. D., Nikara, T. & Bishop, P.O. (1968). Binocular interaction on single units in cat striate cortex. Simultaneous stimulation by single moving slits with receptive fields in correspondence. *Experimental Brain Research*, 6, 391–410.
- Rodman, H. R. & Albright, T. D. (1987). Coding of visual stimulus velocity in area MT of the macaque. *Vision Research*, 27, 2035–2048.
- Sciar, G., Lennie, P. & DePriest, D. D. (1989). Contrast adaptation in striate cortex of macaque. *Vision Research*, 29, 747–755.
- Tootell, R. B. H., Hamilton, S. L. & Switkes, E. (1988). Functional anatomy of macaque striate cortex. IV. Contrast and magno-parvo streams. *Journal of Neuroscience*, 8, 1594–1609.
- Van Essen, D. C., Maunsell, J. H. R. & Bixby, J. L. (1981). The middle temporal visual area in the macaque: Myeloarchitecture, connections, functional properties and topographic organization. *Journal of Comparative Neurology*, 199, 293–326.
- Van Essen, D. C., Newsome, W. T. & Maunsell, J. H. R. (1984). The visual representation in striate cortex of the macaque monkey: Asymmetries, anisotropies and individual variability. *Vision Research*, 24, 429–448.
- Zeki, S. M. (1974). Cells responding to changing image size and disparity in cortex of the rhesus monkey. *Journal of Physiology, London*, 242, 827–841.